Scientific Research Publishing

Advances in Microbiology, 2023, 13, 119-147
https://www.scirp.org/journal/aim
ISSN Online: 2165-3410
ISSN Print: 2165-3402

A New Technique for Use in Culturing Prokaryotes Comprising the Mouse Intestinal Microbiome

Everest Uriel Castaneda[1,2*], Kelly Carroll[1,2], Janice Speshock[1#], Jeff Brady[2]

[1]Department of Biological Sciences, Tarleton State University, Stephenville, Texas, USA
[2]Texas A&M AgriLife Research and Extension Center, Stephenville, Texas, USA
Email: [#]Speshock@Tarleton.edu

How to cite this paper: Castaneda, E.U., Carroll, K., Speshock, J. and Brady, J. (2023) A New Technique for Use in Culturing Prokaryotes Comprising the Mouse Intestinal Microbiome. *Advances in Microbiology*, **13**, 119-147.
https://doi.org/10.4236/aim.2023.133008

Received: December 6, 2022
Accepted: February 27, 2023
Published: March 2, 2023

Abstract

The microbiome has a profound impact on host fitness. pH, oxygen, nutrients, or other factors such as food or pharmaceuticals, subject the microbiome to variations in the gastrointestinal tract. This variation is a cause for concern given dysbiosis of the microbiome is correlated with various disease states. Currently, much research relies on model organisms to study microbial communities since intact microbiomes are challenging to utilize. The objective of this study is to culture an explanted colon microbiome of 4 Balb/c mice to develop an *in vitro* tool for future microbiome studies. We cultured homogenates of the distal colons of 4 mice in trans-well culture dishes. These dishes were incubated for 24 hours in two different oxygen concentration levels and the pH was compared before and after incubation of the cultures. To analyze the integrity of the microbiome, we utilized massively paralleled DNA sequencing with 16S metagenomics to characterize fecal and colon samples to speculate whether future studies may utilize feces in constructing an *in vitro* microbial community to spare animal lives. We found that pH and familial relationships had a profound impact on community structure while oxygen did not have a significant influence. The feces and the colon were similar in community profiles, which lends credence to utilizing feces in future studies. The gut microbiome is of great interest and great importance for studies in a variety of different diseases. Many laboratories do not have access to germ-free mice, which is one optimal way to study mammalian microbiomes, but this technique allowed for the *in vitro* culturing of a majority of the prokaryotes isolated from the colons of mice. This may allow an alternative to study the interactions of this very diverse population of microorganisms without the need for germ-free conditions.

*First author.
#Corresponding author.

Keywords

Microbiome, *ex vivo*, Massively Paralleled Sequencing, pH, Oxygen

1. Introduction

The gastrointestinal (GI) tract of multicellular eukaryotic organisms contains an assortment of diverse microbes and their associated genes, which is defined as the microbiome [1]. Within this system, the GI tract is extremely dynamic due to the interactions between the host and the microbes [2]. The dynamic nature of the GI tract is further confounded by the fact that it does not contain a uniform level of oxygen, temperature, or pH throughout [2] [3]. As a result of the robust variability of the GI tract, the microbiome is known to be highly specific, highly transient, and highly variable between individual organisms [4] [5]. Although the host's core microbiome is relatively stable [6], there are many transient microbial species due to variations in age, diet, or health that differ from host to host [5] [7] [8].

The microbiome forms a symbiotic relationship with its host, and impacts metabolism, response to nutrients, and physiological and immunological development [9]. Essentially, microbes have a cooperative role in the GI tract and contribute to a host's immune system and metabolism [10] [11] [12] [13] with Firmicutes and Bacteroidetes being the predominant Gram-positive and Gram-negative phyla, respectively [9]. Although the natural relationship between the microbiome and the host is essential, overpopulation by an undesirable species, or dysbiosis, has been linked to particular diseases and phenomena such as autism spectrum disorder [14], cancer [11], and obesity [15].

Research is needed to investigate the interactions of the microorganisms of the microbiome and how various stimuli affect them, but many of the species cannot persist in culture [16] [17]. Therefore, most research currently relies on germ-free mice for microbiome studies, which can be cost-prohibitive for many laboratories [15] [18]. One consideration worth noting is the financial burden of raising, sacrificing, and housing vertebrate animals; therefore, it would be beneficial to develop techniques to save organisms and further decrease costs. To begin assessing the transient mixture of microbiota [19], scientists have been utilizing culture-independent, massively parallel sequencing to inquire about shifts within the microbiome and what stimuli affect these changes in composition [20]. With the decreasing cost of DNA sequencing, an influx of research has been possible in this area [21], however, there are still limitations to using strictly genomic sequencing so the culturing of organisms from the microbiome would still be beneficial. In this study, we adapted a 3D culture model from eukaryotic cell culture systems [22] [23] to culture and maintain prokaryotic cultures from the GI microbiomes of four laboratory-bred female Balb/c mice in three-dimensional (3D) well plates, placed into 2 oxygen levels. The distal colons of the mice were homogenized and added to culture air-lift transwell systems

with standard cell culture media and incubated for 24 hours to determine viability and microbiome stability. Due to the variable nature of the oxygen levels of the GI tract [3], we cultured 3D plates in both a conventional incubator and an anaerobic chamber, both at 37 degrees Celsius. Additionally, we attempted to determine the microbial composition of the mouse stool and the distal colon to observe if future studies may utilize feces and avoid sacrificing organisms altogether. We employed massively parallel DNA sequencing to verify final proportional community composition of each sample.

2. Materials and Methods

2.1. Mice

The study was performed under a protocol approved by the Tarleton State University Institutional Animal Care and Usage Committee (Animal Use Protocol 12-009-2016-A1). Four Balb/c females 8 weeks in age were utilized in this experiment. Females were housed together and raised on similar chow diets and similarly weaned. Mice 1 and 2 were siblings while mice 3 and 4 were siblings. All mice were euthanized with 150 microliters of sodium pentobarbital delivered intraperitoneally. Post injection, mice shed two to three samples of stool which were recovered utilizing sterile forceps and immediately frozen. Once deceased, 2.5 cm of the large distal colon from each mouse was removed. After, two small additional 0.5 cm samples of the large distal colon were excised from the specimen and immediately frozen. Colon tissue extractions were added to a sterile tissue grinder along with 5 mL of Dulbecco's Modified Eagle Medium (DMEM; VWR, Radnor, PA). The sample was manually homogenized into a liquid solution.

2.2. Culture Methods

Hydrogel (Corning, Corning, NY) was prepared using 8 mL of molecular grade water and 20 microliters of hydrogel to create a 0.25% solution. 150 microliters of the prepared solution were added to 6.5 mm transwell inserts (n = 8; Corning, Corning, NY) that were placed into a 24 well tissue culture plate (Corning, Corning, NY). In addition, 500 microliters of supplementary Dulbecco's Modified Eagle Medium (DMEM) was added under each well insert. Once the culture plates were prepared, 250 microliters of the homogenized colon were added to the top of the hydrogel in the transwell inserts [22] [23]. Plates were checked for baseline pH by transferring a small drop of medium with a mechanical pipette onto litmus paper. The plates were then added to a single incubator, but to create an anoxic environment, plates were incubated in an anaerobic system (BD Diagnostics, Franklin Lakes, NY). Plates were incubated for 24 hours. The medium below each insert was again tested for pH again and the culture was transferred into sterile 2.5 mL storage tubes and frozen for future DNA extraction.

2.3. DNA Extraction and Library Production

DNA was extracted from each sample using a modified protocol from Brady *et*

al. [24]. After extraction, DNA was amplified utilizing prokaryote specific primers, 519F 5'-CAGCMGCCGCGGTAA-3') and 785R (5'-TACNVGGGTATCTAATCC-3'), that target the V4 region of the 16S rRNA [25] [26]. PCR amplification was accomplished through denaturation at 95˚C for 3 minutes, followed by 35 cycles of 95˚C for 10 seconds, 55˚C for 30 seconds, and 72˚C for 30 seconds. DNA barcodes were added to samples with 10 cycles of the same PCR protocol. To prevent inhibition during PCR, samples underwent an additional cleanup with 20% Chelex 100. Sequences were size-selected with a Pippin Prep instrument (Sage Science, Beverly, MA) to a length of 300 - 600 base pairs. Sequencing was conducted on the Illumina MiSeq platform using 600 cycle paired end v3 sequencing kits at the Texas A&M University Genomics Core Facility. Raw sequences were processed through QIIME [27] and USEARCH [28]. Taxonomy was assigned using Greengenes 13.8 database [29] as a reference with UCLUST [28], and OTU picking was conducted at 97% sequence similarity with the RDP [30] method in QIIME.

The microbes from four mouse distal colons were cultured in 12 cell culture lift inserts in a 24 well plate system. Additionally, a total of 9 fecal and 9 colon samples distributed across 4 mice were prepared for DNA extraction. Due limited spacing in the 96 well plate DNA extraction method, only one colon and fecal sample could be performed in triplicate, and it was randomly selected to be mouse 3.

2.4. Statistical Analysis

Cumulative sum scaling was used to normalize the data and account for uneven sequencing depth between samples [31]. Biom files were constructed through QIIME and transferred into R [32] for further statistical analysis. Phyloseq [33], ggplot2 [34], and vegan [35] packages were utilized to evaluate alpha and beta diversity with seed set at 1400. Alpha diversity was assessed using the Shannon diversity index. Variation in alpha diversity for oxygen, pH, mouse, feces, and colon comparisons were first checked for normality using the Shapiro-Wilk test for normality [36]. The data was non-normal in distribution (Shapiro-Wilk test, $w = 0.9506$, $p < 0.01$); therefore, comparisons were made with non-parametric tests. All multivariate tests were corrected using false discovery rate (FDR) [31]. Comparisons of alpha diversity were assessed using Kruskal Wallis one-way analysis of variance (KW ANOVA) or Wilcoxon rank sums test (Wilcoxon test) while comparisons of beta diversity were assessed with unweighted unifrac distance metrics at 1000 permutations using permutational multivariate analysis of variance (PERMANOVA). Dunn's test post-hoc analysis was done through the dunn.test package in R [37]. In addition, non-parametric t-tests were used for comparisons of mean abundance in individual bacterial strains between samples. A microbial network was constructed using the Co-occurrence Network Interferences (CoNet) application for Cytoscape [38]. Feces and colon data were removed before CoNet analysis. CoNet has been utilized in previous studies to in-

vestigate defined interactions between microbes [39] [40]. Spearman correlation coefficient with a cutoff ratio of 0.6 was utilized, and to focus the network, only microbes with sequence counts greater or equal to 20 were included. 1000 permutations were accomplished through a bootstrapping method with an FDR correction [40].

3. Results

3.1. pH and Oxygen

pH readings of each plate were taken before and after incubation. As shown in Table 1, pH fluctuated from the original baseline of 8. In addition, mice maintained varying levels of pH due to differences in oxygen concentration (Table 1). Sample sizes are uneven due to losses during cleanup or DNA extractions.

3.2. Fecal and Colon Comparison

After quality filtering, we had a total sample size of 111 samples and 3,133,666 sequences total (Supplemental Table S1). The sequence files were submitted to the National Center for Biotechnology Information (NCBI) database (Supplemental Table S2). The profile of the feces and the colon were characterized for microbial composition at the phylum (Figure 1(A)) and family (Figure 1(B)) levels. There was some variation between samples, even within the same mouse, but the core phylum composition of the colon and fecal samples was dominated by Firmicutes and Bacteroidetes (Figure 1(A)), with means of 47% and 49%, respectively, and standard deviations (SD) of 23%. In addition, the family S24-7 (order Bacteroidales) was highly abundant in all samples with a mean of 42% and a SD of 20% (Figure 1(B)). Analysis of beta diversity for each of the feces and colon samples revealed no difference in composition (Supplemental Table S3), and analysis of alpha (Shannon) diversity (Figure 1(C)) also revealed no difference (KW ANOVA $P = 0.47$). Therefore, samples were pooled together for comparison between feces and colon. Shannon diversity index was utilized for comparison of the bulk samples (Figure 1(D)). Results showed no difference

Table 1. pH and oxygen level per sample.

Mouse	Sample Size (n)	Oxygen Level	Plate Baseline pH	Plate Final pH
M1	12	20%	8	10
	11	0%	8	9
M2	11	20%	8	10
	12	0%	8	9
M3	12	20%	8	7
	11	0%	8	6
M4	12	20%	8	7
	12	0%	8	6

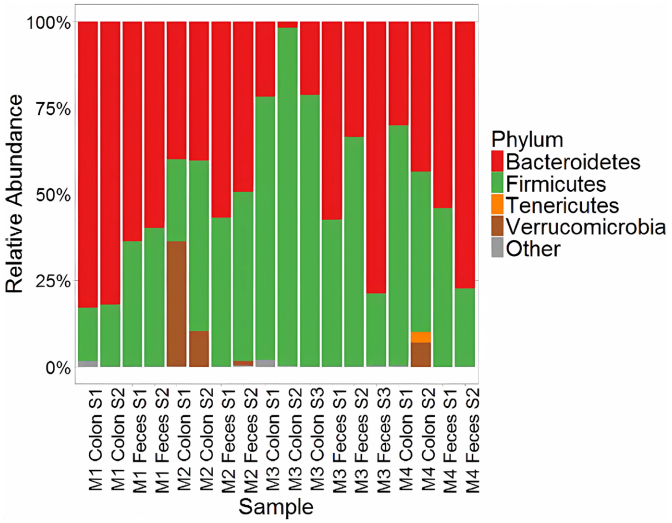
100%
75%
50%
25%
0%
Relative Abundance
Phylum
Bacteroidetes
Firmicutes
Tenericutes
Verrucomicrobia
Other
M1 Colon S1
M1 Colon S2
M1 Feces S1
M1 Feces S2
M2 Colon S1
M2 Colon S2
M2 Feces S1
M2 Feces S2
M3 Colon S1
M3 Colon S2
M3 Colon S3
M3 Feces S1
M3 Feces S2
M3 Feces S3
M4 Colon S1
M4 Colon S2
M4 Feces S1
M4 Feces S2
Sample

(A)

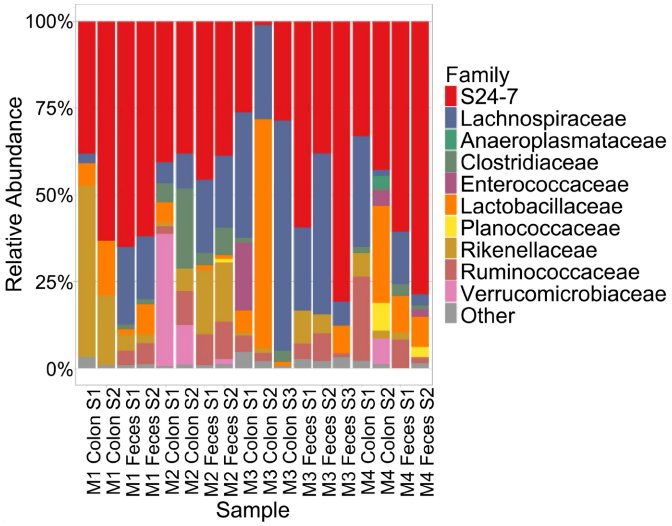
100%
75%
50%
25%
0%
Relative Abundance
Family
S24-7
Lachnospiraceae
Anaeroplasmataceae
Clostridiaceae
Enterococcaceae
Lactobacillaceae
Planococcaceae
Rikenellaceae
Ruminococcaceae
Verrucomicrobiaceae
Other
M1 Colon S1
M1 Colon S2
M1 Feces S1
M1 Feces S2
M2 Colon S1
M2 Colon S2
M2 Feces S1
M2 Feces S2
M3 Colon S1
M3 Colon S2
M3 Colon S3
M3 Feces S1
M3 Feces S2
M3 Feces S3
M4 Colon S1
M4 Colon S2
M4 Feces S1
M4 Feces S2
Sample

(B)

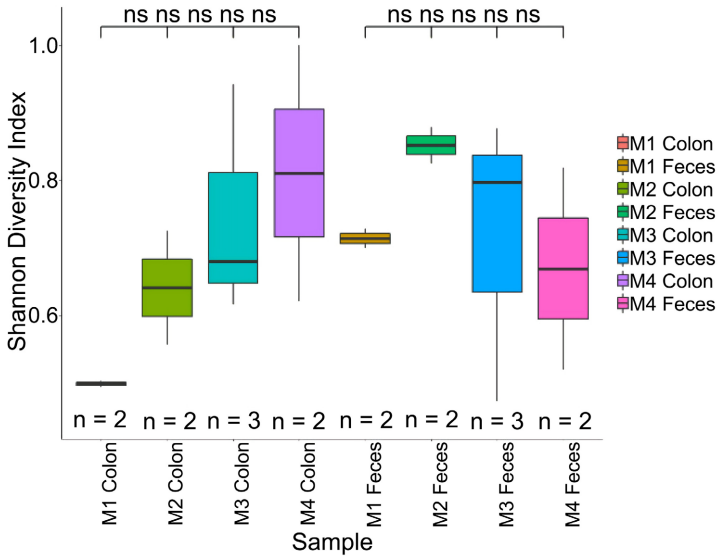
ns ns ns ns ns
ns ns ns ns ns
1.0
0.8
0.6
Shannon Diversity Index
n = 2
n = 2
n = 3
n = 2
n = 2
n = 2
n = 3
n = 2
M1 Colon
M2 Colon
M3 Colon
M4 Colon
M1 Feces
M2 Feces
M3 Feces
M4 Feces
Sample

(C)

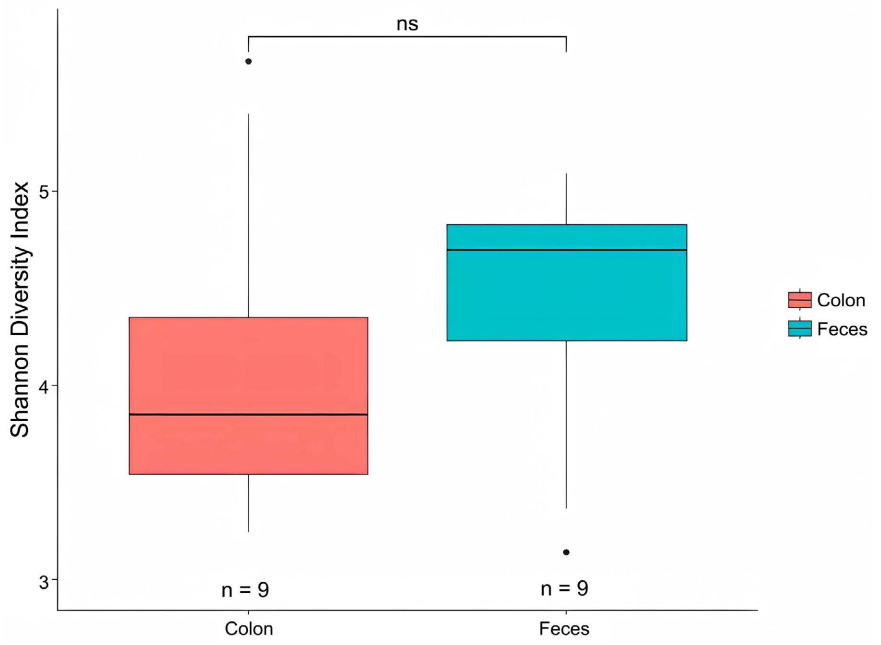

(D)

Figure 1. Community composition of fecal and colon samples. Individual mouse (M) colon and fecal samples (S) with relative abundance at the phylum (A) and family (B) levels, with observations less than 1% pooled into "Other" category. A comparison of Shannon diversity using individual (C) and pooled (D) feces and colon samples illustrates similarities and differences among samples.

between the pooled feces and colon samples (Wilcoxon test, $P = 0.44$). In addition, beta diversity comparison of pooled samples showed no difference (*data not shown*, PERMANOVA, pseudo-F = 1.06, $P = 0.37$). Since it was determined that feces and colon samples are similar, all samples were pooled into one bulk sample, named "pooled microbiome", for diversity comparisons with cultured prokaryotes.

3.3. Microbiome Comparison

In the cultured samples with 24-hour incubation, Firmicutes and Bacteroidetes were the dominant phyla (**Figure 2(A)**). Firmicutes had the highest average relative abundance, 70% (SD 28%), with Bacteroidetes averaging 18% (SD 16%). Mice 1 and 2 exhibited more species richness in the cultures than mice 3 and 4 at the phylum level (**Figure 2(A)**). Across all cultures, the impacts of oxygen levels were not evident at the phylum level (**Figure 2(A)**), at the genus level differences were observed in transient genera (data not shown), although these differences were not significant (**Figure 2(B)**). Shannon diversity index shows a difference between some of the cultures and the colon and fecal microbiome of the mice (KW ANOVA, Dunn's test, **Figure 2(B)**). Post-hoc analysis shows that, compared to the microbiome, mouse cultures 1 and 2 were statistically similar to the pooled microbiome from colon and fecal isolates while mouse cultures 3 and 4 differed significantly (**Supplemental Table S4**, **Figure 2(B)**).

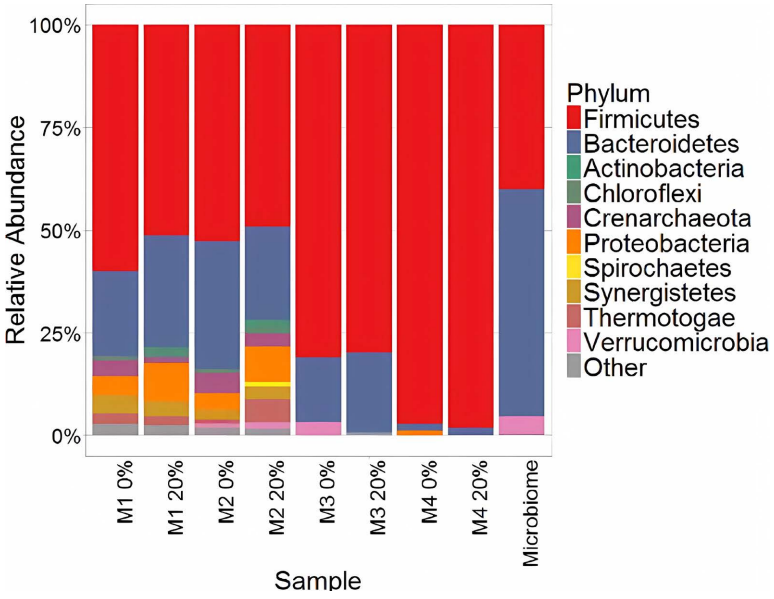

(A)

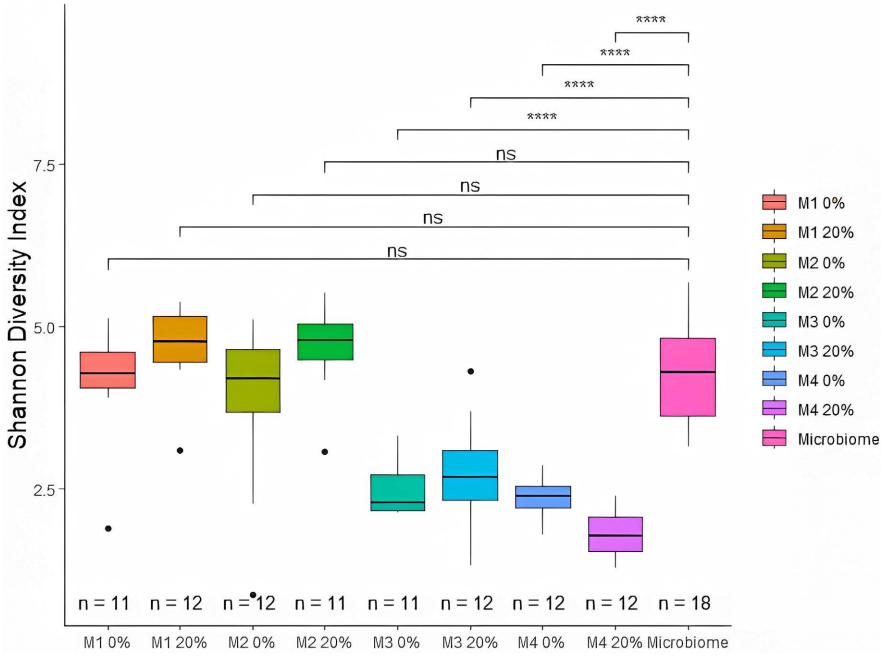

(B)

Figure 2. Community composition of cultures and comparison of pooled microbiome. Cultured prokaryotes from mice (M) at 0 or 20% oxygen tolerance have few differences in relative abundance at the phylum (A) level, with observations less than 1% pooled into "Other" category. Post-hoc, Shannon Diversity, pairwise comparison between cultured samples and the pooled colon microbiome (B) demonstrated that mice 1 and 2 are more representative than mice 3 and 4, $P < 0.05$ is noted by "*", $P < 0.0001$ is noted by "****", and non-significance is noted by "ns."

3.4. Environmental Variables

A community profile of cultural composition due to varying levels of oxygen and pH exposure was constructed (**Figures 3(A)-(D)**). The cultures were placed

overnight into aerobic (20%) or anoxic (0%) conditions, and the dominant bacteria in the cultures produced pH shifts. The overnight culture of colon samples from mice 3 and 4 resulted in a final pH between 6 - 7 (Table 1) and the cultures are dominated by Firmicutes and Bacteroidetes with few transient phyla (Figure 3(A)). The overnight incubation of the cultures from mice 1 and 2 resulted in a higher final pH (9 - 10; Table 1) which resulted in more observed phyla (Figure 3(A)), and these cultures were more representative of the *in vivo* microbiome (Figure 2(B)). Comparison of Shannon diversity revealed that variation in pH led to significant differences in alpha diversity (KW ANOVA, Dunn's test). Post-hoc

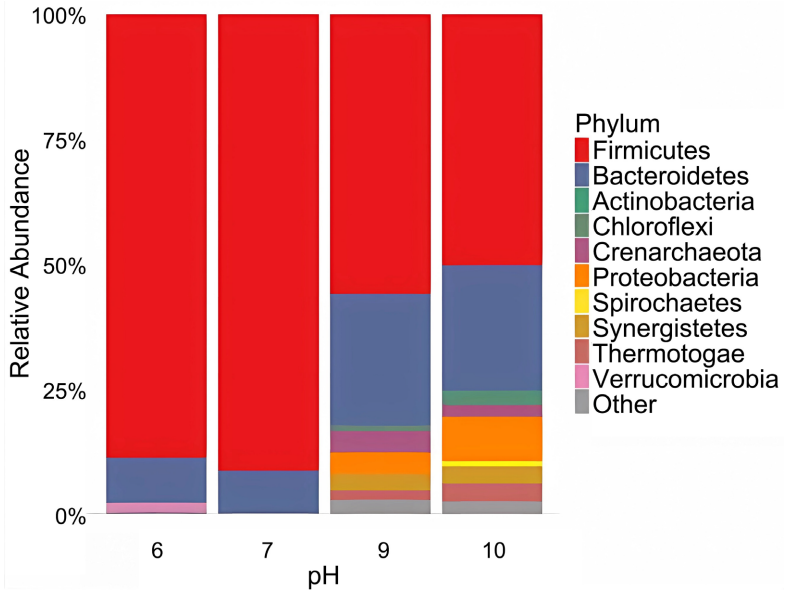

(A)

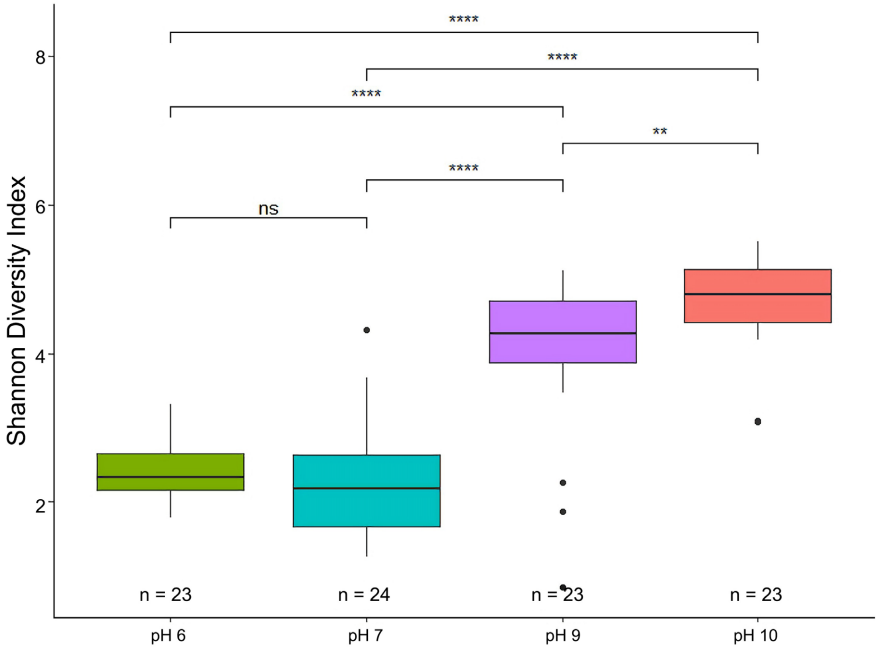

(B)

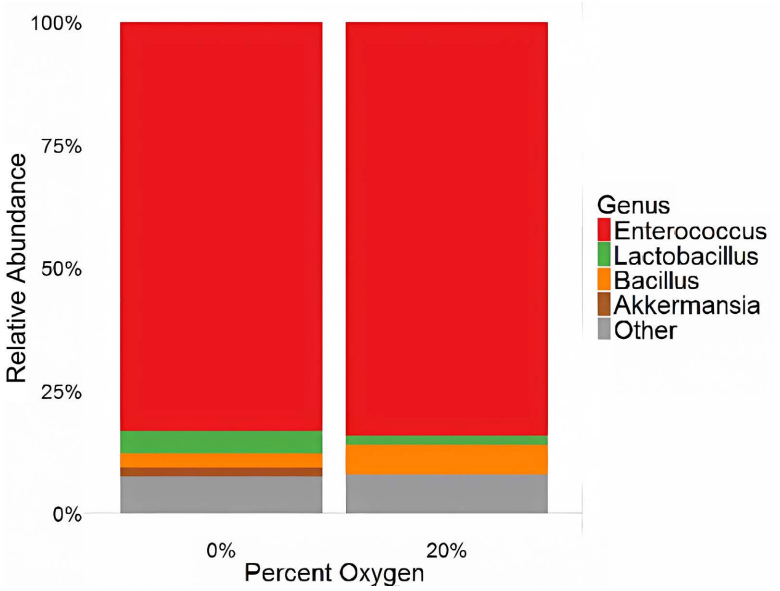

(C)

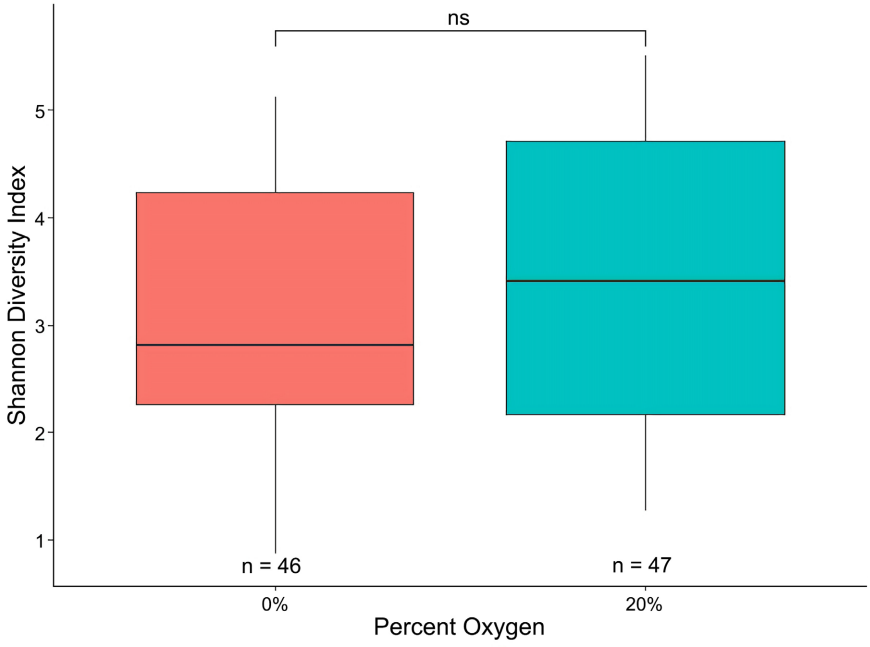

(D)

Figure 3. Microbial community responses to oxygen and pH. The impact of pH was assessed through relative abundance of phyla (A) and a Shannon diversity comparison (B). The impact of oxygen level was assessed through relative abundance of genera (C) and a Shannon diversity comparison (D). Taxa with observations less than 1% are pooled into "Other" category. $P < 0.05$ is noted by "*", $P < 0.0001$ is noted by "****", non-significance is shown by "ns."

analysis revealed that plates reaching a pH of 6 and 7 were similar while all other comparisons differed (**Figure 3(B)**). Analysis of beta diversity also revealed differences in prokaryotic communities between plates of varying pH levels (**Supplemental Table S5**).

When samples cultured at identical oxygen concentration were pooled together, no difference in alpha diversity existed between the two oxygen levels among genera (Wilcoxon test, $P = 0.34$; Figure 3(C), Figure 3(D). However, shifts in the individual mice can be noted, especially with between the two oxygen concentrations. Additionally, distance-based linear modeling revealed that oxygen did not contribute significantly to community clustering (Supplemental Table S6).

3.5. Siblings

Mice 1 and 2 were a sibling pair. Mice 3 and 4 were a sibling pair. A marked difference in prokaryote cultural composition was noted by familial relationship (Supplemental Table S7, Figure 4, Figure 5(A), Figure 5(B)). Mice 1 and 2 had greater diversity in their cultures than mice 3 and 4 (Figure 5(A)). Mouse 1 had much higher *Lactobacillus*, HA73 (Phylum Synergistetes), and *Ruminofilibacter* than mice 3 and 4 (Figure 5(B)) and mouse 2 had even more diversity with increases in the genus *Clostridium* (Figure 5(B)). Sibling relationship explains the changes in community composition as time elapsed in the incubators (Supplemental Table S6). Distance-based linear modeling indicated pH, individual mouse, and sibling effects all significantly contributed to microbial community variation when considered independently ($P < 0.001$), accounting for 20%, 18%, and 22% of the variation, respectively, while oxygen level did not impact the microbiota (Supplemental Table S6). However, when these variables were considered together, a most parsimonious model containing individual

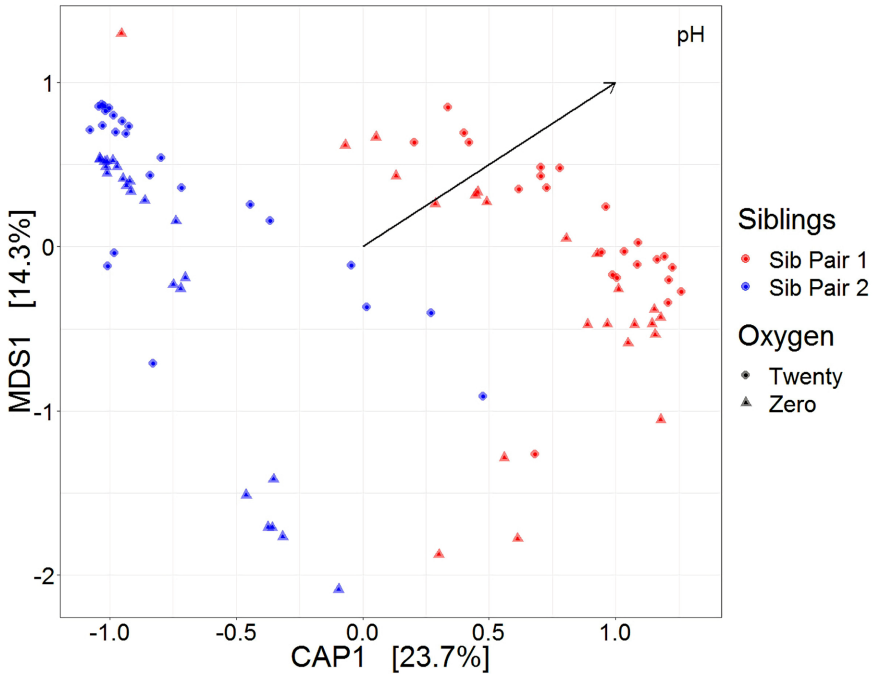

Figure 4. CCA for the effects of pH, oxygen, and sibling relationship on community structuring. Data was first square-root transformed and then ordinated by Bray-Curtis distance metric.

mouse and sibling relationship accounted for 29.0% of the variation while pH did not contribute to explaining microbial variation if individual mouse and sibling relationship were already in the model. Additionally, Shannon diversity significantly varied between sibling groups (KW ANOVA, $P < 0.01$). Post-hoc analysis showed mouse 1 and mouse 2 were similar and varied from mouse 3 and mouse 4, which were also similar (Dunn's test, **Supplemental Table S4** and **Figure 5(C)**). Additionally, beta diversity varied according to familial relationship (PERMANOVA, $P < 0.01$).

3.6. Microbial Network

The OTUs in the microbial network represent 88% of the relative sequence count for the cultured well plates (**Figure 6**). Many of the interactions were positive in

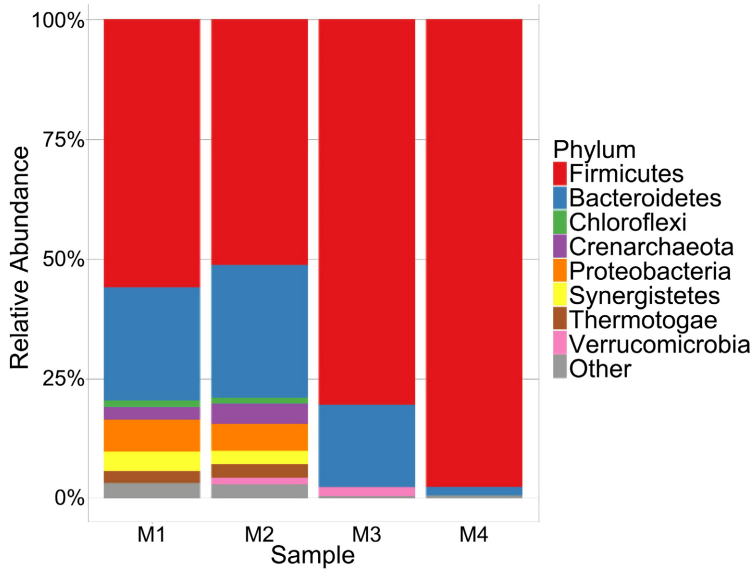

(A)

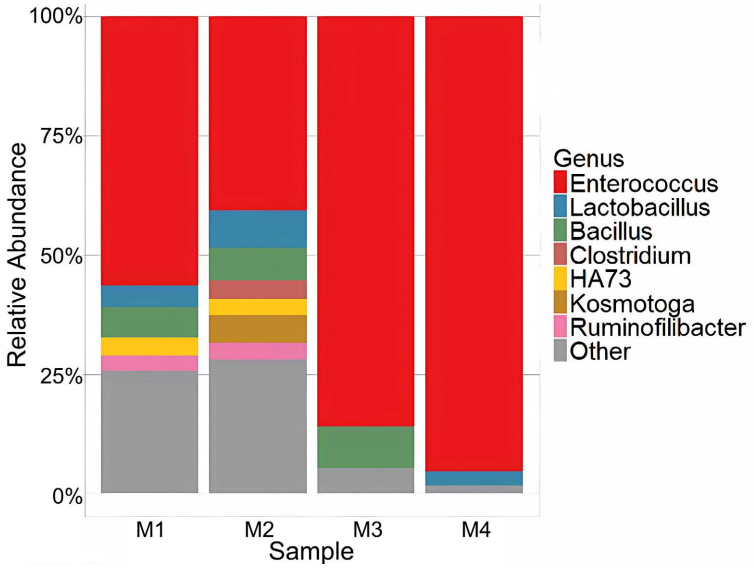

(B)

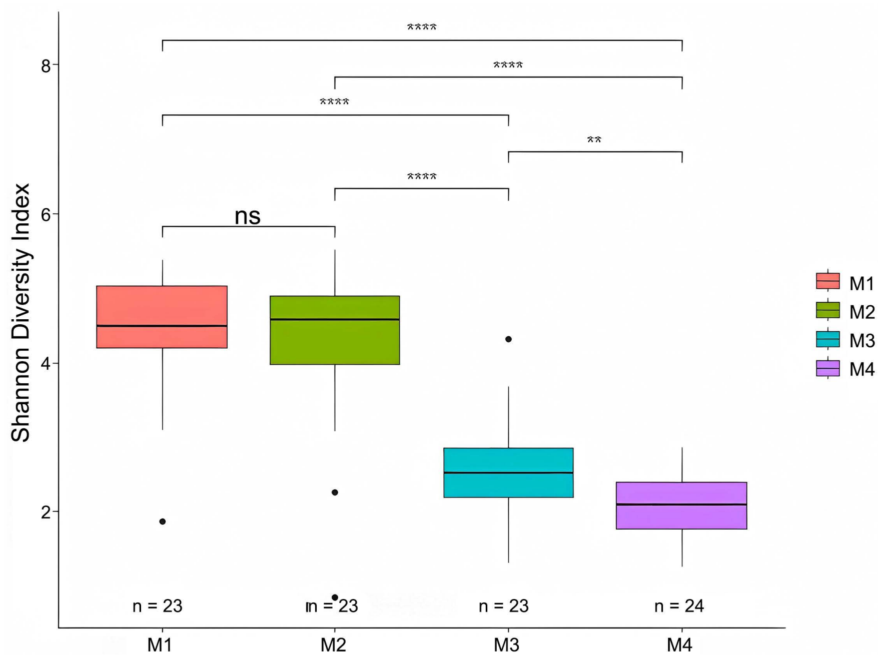

(C)

Figure 5. Microbial composition by mouse. Relative abundance of bacteria phyla (A) and genera (B). Observations less than 0.03% are pooled into "Other" category. (C) Shannon diversity index comparison using mouse 2 as a reference group. "****" means significant at $P < 0.0001$ while "ns" means non-significant.

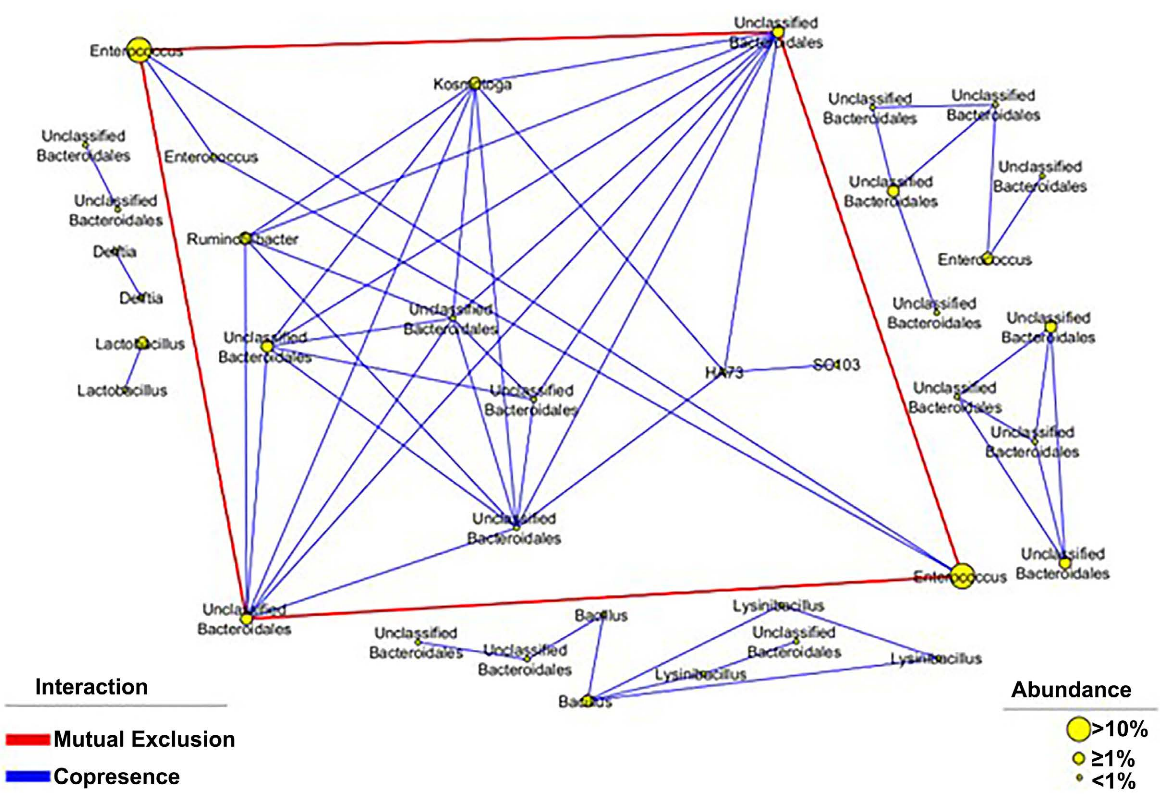

Figure 6. Microbial network generated using Spearman's rank correlation at the taxonomic level of genus. Most of the edges, 54 of 58, are of a positive correlation. The rest are negative.

nature meaning co-presence in a shared-niche is the most abundant interaction type. Negative, mutually exclusive interactions are only between the microbial genus *Enterococcus* and an unclassified strain of Bacteroidales (Figure 5). The interaction between the 4 mutually exclusive OTUs account for 50% of all sequences. *Enterococcus* species were more well represented in the cultured samples than the colon and fecal samples ("pooled microbiome"), especially in cultures from mice 3 and 4 (Figure 7(A); Supplemental Table S8), which had the lower pH (Table 1, Figure 7(B)). The low pH of these cultures may be influenced by an increase in *Lactobacillus* (Figure 7(C)). The increase in *Enterococcus* and *Lactobacillus* in mice 3 and 4 resulted in a decline in genera from the phylum Proteobacteria (Figure 7(D), Supplemental Table S9). Although perhaps not proportional to the *in vivo* colonic microbiome, most representative

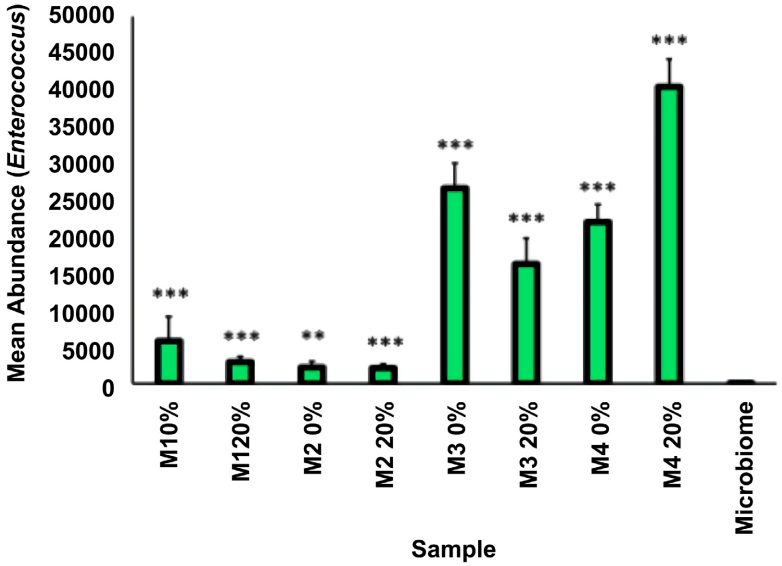

(A)

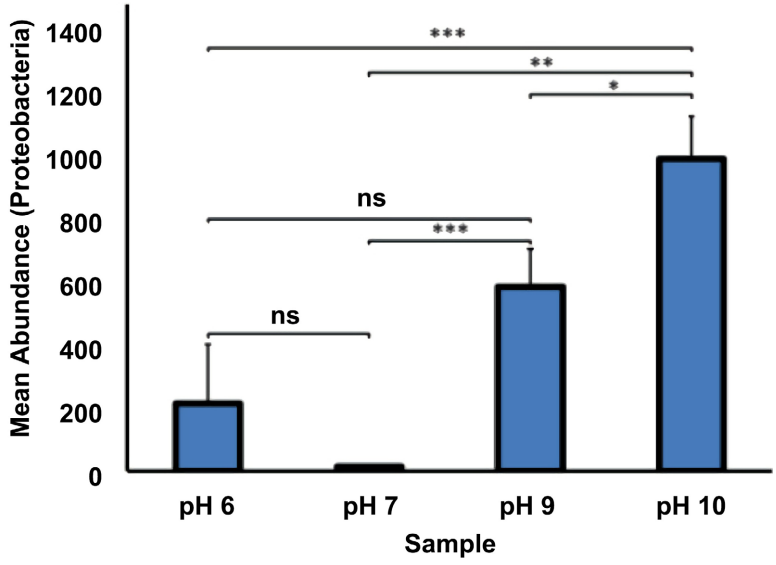

(B)

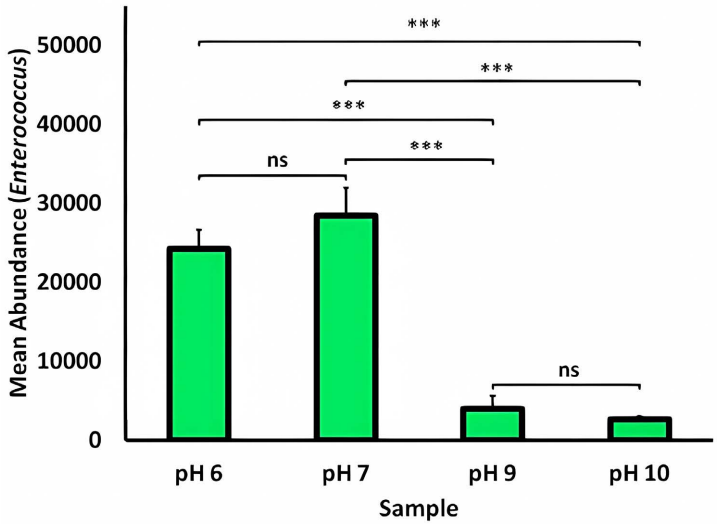
Mean Abundance (*Enterococcus*)
50000
40000
30000
20000
10000
0
***
***
***
***
ns
ns
pH 6
pH 7
pH 9
pH 10
Sample

(C)

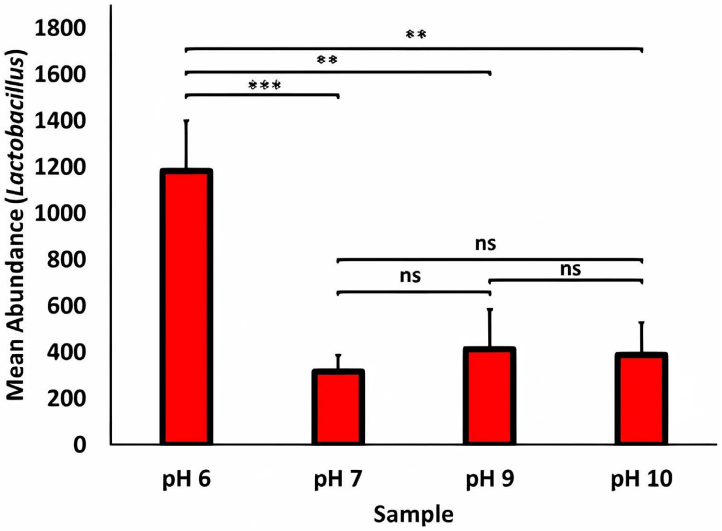
Mean Abundance (*Lactobacillus*)
1800
1600
1400
1200
1000
800
600
400
200
0
**
**
***
ns
ns
ns
pH 6
pH 7
pH 9
pH 10
Sample

(D)

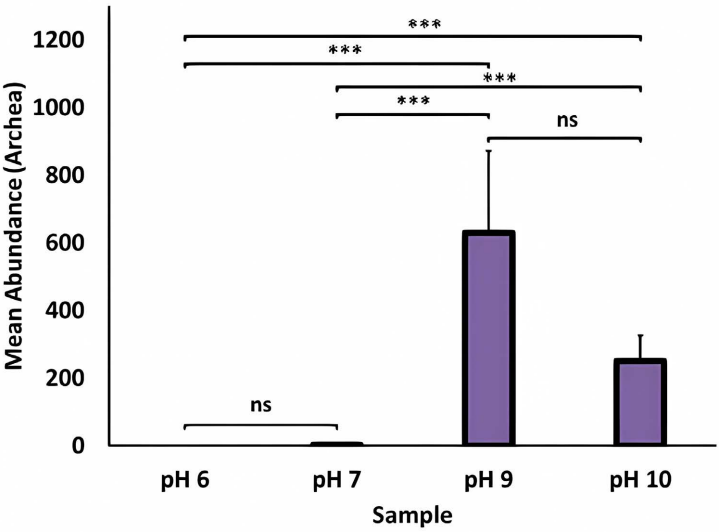
Mean Abundance (Archea)
1200
1000
800
600
400
200
0
***
***
***
***
ns
ns
pH 6
pH 7
pH 9
pH 10
Sample

(E)

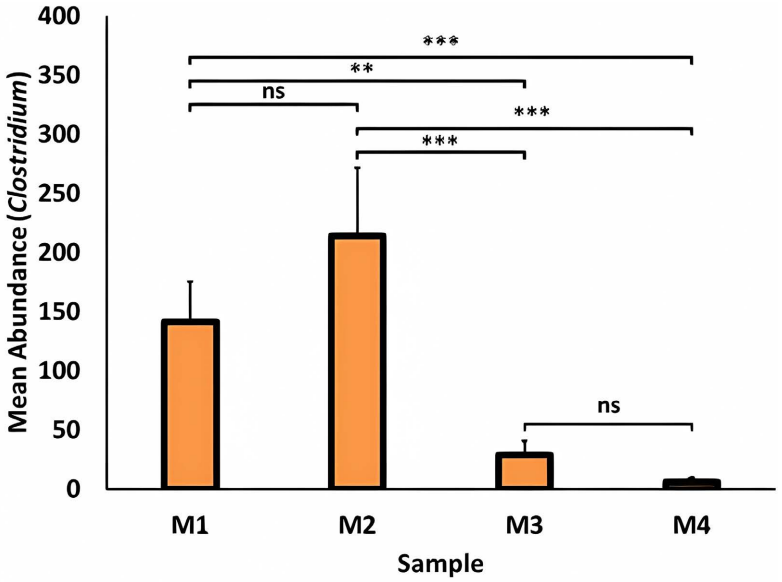

(F)

Figure 7. Comparative mean abundance of individual microbial taxa. (A) Comparison of the mean abundance of *Enterococcus* in cultured plates compared to the microbiome. (B) Comparison of the mean abundance of *Enterococcus* in plates reaching varying pH levels. (C) Comparison of mean abundance of *Lactobacillus* in plates reaching varying pH levels. (D) Comparison of mean abundance of Proteobacteria in plates reaching varying pH levels. (E) Comparison in mean abundance of Archaea in plates reaching varying pH levels. (F) Comparison in mean abundance of *Clostridium* in plates reaching varying pH levels. "ns", non-significant; "***", $P < 0.001$; "**", $P < 0.01$; "*", $P < 0.05$.

prokaryotes, including the hard to grow Archaea (**Figure 7(E)**) and *Clostridium* (**Figure 7(F)**) were isolated from these cultures. The addition of the chemical propidium monoazide (PMA) to the preparations indicated that the cultures were not just present, but also alive, as no significant differences were observed with or without PMA treatment at the level of family (**Figure 8(A)**). To conclude, the stability of the cultures was confirmed when a plate of eight transwells were frozen for one month at −80˚C, and again there were no statistically significant changes in the cultures at the level of family (**Figure 8(B)**).

4. Discussion

Current studies of the microbiome utilize germ-free mice, which are expensive to house and breed [20]. In this study, we attempted to culture a representative population of prokaryotes from the distal colon in 3D transwell culture plates to allow for an alternative for product testing prior to the germ-free animals. We found that oxygen level had little impact, but ultimately the population of microbes at the initiation of cultures, which contributes to the stability of pH, impacted the ability to culture (**Figure 2**, **Figure 3**). Cultures for mouse 1 and 2 were comparable in alpha diversity to the microbial population of the colon and feces (**Supplemental Table S4**, **Supplemental Table S5**, **Figure 2(B)**), which is very promising, and these microbes produced a pH of 9 - 10 when cultured (**Table 1**).

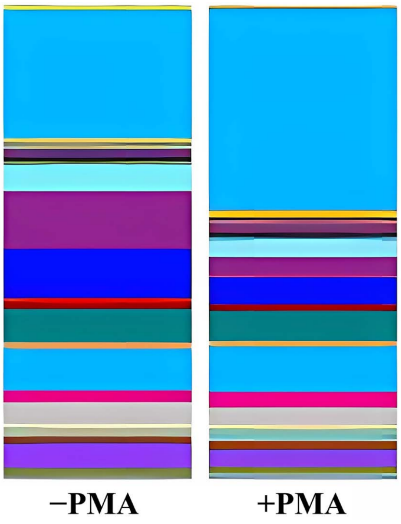

(A)

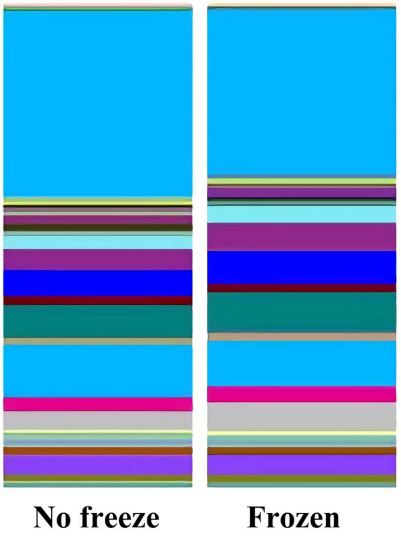

(B)

Figure 8. Taxa summary plots compiled. The cultures from the mice were subjected to treatment with PMA (A) or were frozen (B) to determine culture stability. There is no statistical difference between either of these comparisons.

These cultures contained a high percentage of Bacteroidetes and Firmicutes (**Figure 2(A)**), which is consistent with recent data on the colon microbe populations in mammals [9] [41] [42] [43], along with some other minor phyla (**Figure 2(A)**). Some factors, most likely bacterial, caused the pH of the cultures from mice 3 and 4 to decline from baseline to 6 - 7 (**Table 1**). This low pH dramatically altered the cultures obtained from the colon samples of these animals (**Figure 2**, **Figure 3**), and they were less consistent with the normal GI microflora of animals [42]. The cultures from mice 3 and 4 were predominantly Firmicutes, with a smaller percentage of Bacteroidetes.

Although oxygen did not specifically result in significant changes when observed collectively (**Figure 3(C)**, **Figure 3(D)**), it may have been a factor in-

fluencing the pH (**Table 1**). There were different microbes present in the 0% and 20% cultures, and these microbes likely caused a pH shift. For example, *Lactobacillus*, a lactic acid producing bacterial genus, increased in the pH 6 cultures (**Figure 7(C)**), which appeared to be a result of the mice 3 and 4 colon extracts being incubated in the absence of oxygen (**Table 1**). *Lactobacillus spp.* has been shown to grow better in anaerobic conditions [44], leading to increased lactic acid production and lower pH. *Lactobacillus* has also been shown to be present in commercially-available mouse food, and thus feeding selection may impact its presence or absence in the gastrointestinal microbiome [9]. The presence of oxygen also likely affected species from the genus *Enterococcus* as it significantly increased between mice cultures and the pooled microbiome, especially those with a lower pH (**Figure 7(A)**, **Figure 7(B)**; **Supplemental Table S9**). The upsurge of bacteria from the *Enterococcus* genus likely minimized the role of oxygen in incubating these fecal anaerobes. *Enterococcus* is a facultative anaerobe [45]; therefore, since it is a known pioneer colonizer of the GI tract, its presence possibly established the anoxic environment [46]. The presence of oxygen also likely led to the increase in Proteobacteria, as these organisms are often amenable to laboratory culture, and likely have a preference for the incubator (**Figure 2(A)**, **Figure 7(D)**). However, they did appear to be repressed in the lower pH range (**Figure 3(A)**, **Figure 7(D)**), and their presence may have been a factor that contributed to the shift from the distal colon physiological pH of 6.6 - 6.9 [47] to that of 9 - 10. The metabolism of proteins to release amine groups by species of this phylum perhaps led to the increase in pH in these cultures [48]. pH was a strong influence in the growth of Archaea. Few Archaea were observed in the cultures, but those detected grew more readily in plates with a higher pH (**Supplemental Table S9**, **Figure 7(E)**). Not only are Archaea difficult to culture, but also their diversity is not well studied in regard to the gut microbiome [49], making this system a potentially advantageous method to understand their role in the GI tract.

Microbiome acquisition is passed on from mother to litter [18] [50]. Our microbiome cultures were highly impacted by familial relationships (**Supplemental Table S7**). One such example was that the mice differed in the amount of *Clostridium* cultured. Sibling pair mice 1 and 2 had more numerous strains of *Clostridium* than sibling pair mice 3 and 4 (**Supplemental Table S10**, **Figure 7(F)**). Not only were these mice siblings but were also weaned by different mothers. The effects of weaning are similar to Bian *et al.* wherein the abundance of species from the family Clostridiaceae was affected by the nursing mother [51]. Our result not only solidifies the impact of the mother on the microbiome, but also shows this dynamic still occurs even explanted from the source.

Ultimately, we showed that the feces and large distal colon are highly similar; therefore, future experiments may avoid sacrificing mice by culturing feces. Future experiments will need to control for pH to acquire the highest amount of diversity possible, and perhaps use a mixed fecal source to avoid sibling biases.

Since none of the plates maintained the original baseline pH, using a biological buffer may create a closer replica of the microbiome. Even without additional measures for controlling media pH, we have succeeded in creating a method to culture bacteria of the microbiome that are difficult to culture. Ultimately, this study found that pH was a stronger influencer of community composition than oxygen, but it seems as though the oxygen levels led to a proliferation of certain microbes that impacted pH. The microbes in culture impacted the pH of the media, and future goals would be to establish a physiological pH by maintaining the correct proportions of microbes. The use of an anaerobic chamber during necropsy and culture would have likely aided the survival rate of more strict anaerobes, and perhaps limited the Proteobacteria. Additionally, the use of different matrices that might produce a more solidified platform than hydrogel might create more of an anaerobic niche to prevent loss of organisms like the Bacteroidetes, which are mostly strict anaerobes [52].

Ultimately, our culture mimic of the distal colon microbiome did not maintain the full proportions of microbes, but we were able to culture a majority of the prokaryotes of the GI microbiome providing a collection of a diverse number of prokaryotic strains for microbiome analysis. Optimizing efforts in culture media, matrices, fecal extraction, and atmospheric gradients is extremely important in culturing all desired microbes [53]. However, even with this preliminary study, we were able to culture a majority of the prokaryotic microbes of the GI tract, including very-difficult-to-culture strains, for example, Methanobacteria [54], mean of 0.57 (SD 4.31) (**Figure 7(E)**).

Acknowledgements

We would like to thank the staff at Texas A&M AgriLife Research and Extension Center for aiding in the project, the Tarleton State University Office of Student Research and Creative Activities, and the College of Science and Technology for funding this research, and the Tarleton State University College of Graduate Studies for the assistantship for Mr. Castaneda.

Conflicts of Interest

The authors declare no conflicts of interest regarding the publication of this paper.

References

[1] Ursell, L.K., Metcalf, J.L., Parfrey, L.W. and Knight, R. (2012) Defining the Human Microbiome. *Nutrition Reviews*, **70**, S38-S44. https://doi.org/10.1111/j.1753-4887.2012.00493.x

[2] Ilhan, Z.E., Marcus, A.K., Kang, D. and Rittmann, B.E. (2017) pH-Mediated Microbial and Metabolic Interactions in Fecal Enrichment Cultures. *mSphere*, **2**, e00047-17. https://doi.org/10.1128/mSphere.00047-17

[3] Zheng, L., Kelly, C.J. and Colgan, S.P. (2015) Physiologic Hypoxia and Oxygen Homeostasis in the Healthy Intestine. A Review in the Theme: Cellular Responses

to Hypoxia. *American Journal of Physiology-Cell Physiology*, **309**, C350-C360. https://doi.org/10.1152/ajpcell.00191.2015

[4] Turnbaugh, P.J., Hamady, M., Yatsunenko, T., *et al.* (2009) A Core Gut Microbiome in Obese and Lean Twins. *Nature*, **457**, 480-484. https://doi.org/10.1038/nature07540

[5] Huttenhower, C., Gevers, D., Knight, R., *et al.* (2012) Structure, Function and Diversity of the Healthy Human Microbiome. *Nature*, **486**, 207-214. https://doi.org/10.1038/nature11234

[6] Tillisch, K. (2014) The Effects of Gut Microbiota on CNS Function in Humans. *Gut Microbes*, **5**, 404-410. https://doi.org/10.4161/gmic.29232

[7] Engen, P.A., Green, S.J., Voigt, R.M., *et al.* (2015) The Gastrointestinal Microbiome: Alcohol Effects on the Composition of Intestinal Microbiota. *Alcohol Research*, **37**, 223-236.

[8] Nicholson, J.K., Holmes, E., Kinross, J., *et al.* (2012) Host-Gut Microbiota Metabolic Interactions. *Science*, **108**, 1262-1268. https://doi.org/10.1126/science.1223813

[9] Irvin, A., Cockburn, A., Primerano, D., Denvir, J., Boskovic, G., Infante, A., Wu, G. and Cuff, C. (2017) Diet-Induced Alteration of the Murine Intestinal Microbiome Following Antibiotic Ablation. *Advances in Microbiology*, **7**, 545-564. https://doi.org/10.4236/aim.2017.77043

[10] Tourneur, E. and Chassin, C. (2013) Neonatal Immune Adaptation of the Gut and Its Role during Infections. *Clinical and Developmental Immunology*, **2013**, Article ID: 270301. https://doi.org/10.1155/2013/270301

[11] Schwabe, R.F. and Jobin, C. (2013) The Microbiome and Cancer. *Nature Reviews Cancer*, **13**, 800-812. https://doi.org/10.1038/nrc3610

[12] Sommer, F. and Bäckhed, F. (2013) The Gut Microbiota—Masters of Host Development and Physiology. *Nature Reviews Microbiology*, **11**, 227-238. https://doi.org/10.1038/nrmicro2974

[13] Cho, I. and Blaser, M.J. (2012) The Human Microbiome: At the Interface of Health and Disease. *Nature Reviews Genetics*, **13**, 260-270. https://doi.org/10.1038/nrg3182

[14] Li, Q., Han, Y., Dy, A.B.C. and Hagerman, R.J. (2017) The Gut Microbiota and Autism Spectrum Disorders. *Frontiers in Cellular Neuroscience*, **11**, 120. https://doi.org/10.3389/fncel.2017.00120

[15] Turnbaugh, P.J., Bäckhed, F., Fulton, L. and Gordon, J.I. (2008) Diet-Induced Obesity Is Linked to Marked but Reversible Alterations in the Mouse Distal Gut Microbiome. *Cell Host & Microbe*, **3**, 213-223. https://doi.org/10.1016/j.chom.2008.02.015

[16] Lagier, J.C., Khelaifia, S., Alou, M.T., *et al.* (2016) Culture of Previously Uncultured Members of the Human Gut Microbiota by Culturomics. *Nature Microbiology*, **1**, 16203. https://doi.org/10.1038/nmicrobiol.2016.203

[17] Browne, H.P., Forster, S.C., Anonye, B.O., *et al.* (2016) Culturing of "Unculturable" Human Microbiota Reveals Novel Taxa and Extensive Sporulation. *Nature*, **533**, 543-546. https://doi.org/10.1038/nature17645

[18] Ericsson, A.C. and Franklin, C.L. (2015) Manipulating the Gut Microbiota: Methods and Challenges. *ILAR Journal*, **56**, 205-217. https://doi.org/10.1093/ilar/ilv021

[19] Trosvik, P. and Jacques De Muinck, E. (2015) Ecology of Bacteria in the Human Gastrointestinal Tract—Identification of Keystone and Foundation Taxa. *Microbiome*, **3**, 44. https://doi.org/10.1186/s40168-015-0107-4

[20] Goodman, A.L., Kallstrom, G., Faith, J.J., *et al.* (2011) Extensive Personal Human Gut Microbiota Culture Collections Characterized and Manipulated in Gnotobiotic

Mice. *PNAS*, **108**, 6252-6257. https://doi.org/10.1073/pnas.1102938108

[21] Shokralla, S., Spall, J.L., Gibson, J.F. and Hajibabaei, M. (2012) Next-Generation Sequencing Technologies for Environmental DNA Research. *Molecular Ecology*, **21**, 1794-1805. https://doi.org/10.1111/j.1365-294X.2012.05538.x

[22] Murdoch, A.D., Grady, L.M., Ablett, M.P., *et al.* (2007) Chondrogenic Differentiation of Human Bone Marrow Stem Cells in Transwell Cultures: Generation of Scaffold-Free Cartilage. *Stem Cells*, **25**, 2786-2796. https://doi.org/10.1634/stemcells.2007-0374

[23] Tibbitt, M.W. and Anseth, K.S. (2009) Hydrogels as Extracellular Matrix Mimics for 3D Cell Culture. *Biotechnology and Bioengineering*, **103**, 655-663. https://doi.org/10.1002/bit.22361

[24] Brady, J.A., Faske, J.B., Castañeda-Gill, J.M., *et al.* (2011) High-Throughput DNA Isolation Method for Detection of *Xylella fastidiosa* in Plant and Insect Samples. *Journal of Microbiological Methods*, **86**, 310-312. https://doi.org/10.1016/j.mimet.2011.06.007

[25] Herlemann, D.P.R., Labrenz, M., Jürgens, K., *et al.* (2011) Transitions in Bacterial Communities along the 2000 km Salinity Gradient of the Baltic Sea. *The ISME Journal*, **5**, 1571-1579. https://doi.org/10.1038/ismej.2011.41

[26] Klindworth, A., Pruesse, E., Schweer, T., *et al.* (2013) Evaluation of General 16S Ribosomal RNA Gene PCR Primers for Classical and Next-Generation Sequencing-Based Diversity Studies. *Nucleic Acids Research*, **41**, e1. https://doi.org/10.1093/nar/gks808

[27] Caporaso, J.G., Lauber, C.L., Walters, W.A., *et al.* (2011) Global Patterns of 16S rRNA Diversity at a Depth of Millions of Sequences per Sample. *PNAS*, **108**, 4516-4522. https://doi.org/10.1073/pnas.1000080107

[28] Edgar, R.C. (2016) Search and Clustering Orders of Magnitude Faster than BLAST. *Bioinformatics*, **26**, 2460-2461. https://doi.org/10.1093/bioinformatics/btq461

[29] DeSantis, T.Z., Hugenholtz, P., Larsen, N., *et al.* (2006) Green Genes, a Chimera-Checked 16S rRNA Gene Database and Workbench Compatible with ARB. *Applied and Environmental Microbiology*, **72**, 5069-5072. https://doi.org/10.1128/AEM.03006-05

[30] Cole, J.R., Wang, Q., Cardenas, E., *et al.* (2009) The Ribosomal Database Project: Improved Alignments and New Tools for rRNA Analysis. *Nucleic Acids Research*, **37**, 141-145. https://doi.org/10.1093/nar/gkn879

[31] Paulson, J.N., Colin Stine, O., Bravo, H.C. and Pop, M. (2013) Differential Abundance Analysis for Microbial Marker-Gene Surveys. *Nature Methods*, **10**, 1200-1202. https://doi.org/10.1038/nmeth.2658

[32] R Core Team (2018) R: A Language and Environment for Statistical Computing. Vienna. https://www.r-project.org

[33] McMurdie, P.J. and Holmes, S. (2013) Phyloseq: An R Package for Reproducible Interactive Analysis and Graphics of Microbiome Census Data. *PLOS ONE*, **8**, e61217. https://doi.org/10.1371/journal.pone.0061217

[34] Wickham, H. (2009) ggplot2: Elegant Graphics for Data Analysis. Springer, New York. https://doi.org/10.1007/978-0-387-98141-3

[35] Oksanen, J., Kindt, R., Legendre, P., *et al.* (2007) The Vegan Package. *Community Ecology Package*, **10**, 631-637.

[36] Yap, B.W. and Sim, C.H. (2011) Comparisons of Various Types of Normality Tests. *Journal of Statistical Computation and Simulation*, **81**, 2141-2155.

https://doi.org/10.1080/00949655.2010.520163

[37] Dinno, A. (2017) Package "dunn.test". CRAN Repos. 1-7.

[38] Shannon, P., Markiel, A., *et al.* (2003) Cytoscape: A Software Environment for Integrated Models of Biomolecular Interaction Networks. *Genome Research*, **13**, 2498-2504. https://doi.org/10.1101/gr.1239303

[39] Barberán, A., Bates, S.T., Casamayor, E.O. and Fierer, N. (2012) Using Network Analysis to Explore Co-Occurrence Patterns in Soil Microbial Communities. *The ISME Journal*, **6**, 343-351. https://doi.org/10.1038/ismej.2011.119

[40] Faust, K., Sathirapongsasuti, J.F., Izard, J., *et al.* (2012) Microbial Co-Occurrence Relationships in the Human Microbiome. *PLOS Computational Biology*, **8**, e1002606. https://doi.org/10.1371/journal.pcbi.1002606

[41] Weldon, L., Abolins, S., Lenzi, L., *et al.* (2015) The Gut Microbiota of Wild Mice. *PLOS ONE*, **10**, e0134643. https://doi.org/10.1371/journal.pone.0134643

[42] Kreisinger, J., Čížková, D., Vohánka, J. and Piálek, J. (2014) Gastrointestinal Microbiota of Wild and Inbred Individuals of Two House Mouse Subspecies Assessed Using High-Throughput Parallel Pyrosequencing. *Molecular Ecology*, **23**, 5048-5060. https://doi.org/10.1111/mec.12909

[43] Ormerod, K.L., Wood, D.L.A., Lachner, N., *et al.* (2016) Genomic Characterization of the Uncultured Bacteroidales Family S24-7 Inhabiting the Guts of Homeothermic Animals. *Microbiome*, **4**, 36. https://doi.org/10.1186/s40168-016-0181-2

[44] Murphy, M.G. and Condon, S. (1984) Comparison of Aerobic and Anaerobic Growth of *Lactobacillus plantarum* in a Glucose Medium. *Archives of Microbiology*, **138**, 49-53. https://doi.org/10.1007/BF00425406

[45] Fisher, K. and Phillips, C. (2009) The Ecology, Epidemiology and Virulence of Enterococcus. *Microbiology*, **155**, 1749-1757. https://doi.org/10.1099/mic.0.026385-0

[46] Wampach, L., Heintz-Buschart, A., Hogan, A., *et al.* (2017) Colonization and Succession within the Human Gut Microbiome by Archaea, Bacteria, and Microeukaryotes during the First Year of Life. *Frontiers in Microbiology*, **8**, Article No. 738. https://doi.org/10.3389/fmicb.2017.00738

[47] Van Herreweghen, F., Van den Abbeele, P., De Mulder, T., *et al.* (2017) *In Vitro* Colonization of the Distal Colon by *Akkermansia muciniphila* Is Largely Mucin and pH Dependent. *Beneficial Microbes*, **8**, 81-96. https://doi.org/10.3920/BM2016.0013

[48] Busse, H.-J. (2011) Polyamines. In: Rainey, F. and Oren, A., Eds., *Taxonomy of Prokaryotes*, Elsevier, Amsterdam, 239-259. https://doi.org/10.1016/B978-0-12-387730-7.00011-5

[49] Raymann, K., Moeller, A.H. and Goodman, A.L. (2017) Unexplored Archaeal Diversity in the Great Ape Gut Microbiome. *mSphere*, **2**, e00026-17. https://doi.org/10.1128/mSphere.00026-17

[50] Mueller, N.T., Bakacs, E., Combellick, J., *et al.* (2015) The Infant Microbiome Development: Mom Matters. *Trends in Molecular Medicine*, **29**, 109-117. https://doi.org/10.1016/j.molmed.2014.12.002

[51] Bian, G., Ma, S., Zhu, Z., *et al.* (2016) Age, Introduction of Solid Feed and Weaning Are More Important Determinants of Gut Bacterial Succession in Piglets than Breed and Nursing Mother as Revealed by a Reciprocal Cross-Fostering Model. *Environmental Microbiology*, **18**, 1566-1577. https://doi.org/10.1111/1462-2920.13272

[52] Lee, A., Gordon, J., Lee, C.-J. and Dubos, R. (1971) The Mouse Intestinal Microflora with Emphasis on the Strict Anaerobes. *JEM*, **133**, 339-352. https://doi.org/10.1084/jem.133.2.339

[53] Lagier, J., Edouard, S., Pagnier, I., *et al.* (2015) Current and Past Strategies for Bacterial Culture in Clinical Microbiology. *Clinical Microbiology Reviews*, **28**, 208-236. https://doi.org/10.1128/CMR.00110-14

[54] Khelaifia, S., Raoult, D. and Drancourt, M. (2013) A Versatile Medium for Cultivating Methanogenic Archaea. *PLOS ONE*, **8**, e61563. https://doi.org/10.1371/journal.pone.0061563

Supplemental Table

Supplemental Table S1. Sequence count per mouse.

Mouse	Sample Size	Total Sequence Count	Average Sequence Count
M1	27	234,051	8669
M2	27	384,215	14,230
M3	29	1,243,981	40,128
M4	28	1,194,017	45,924

Supplemental Table S2. NCBI database submissions.

Accession	Sample Name	SPUID	Organism	Tax ID	BioProject
SAMN12230199	M1ColonPlate1A2	M1ColonPlate1A2	mouse gut metagenome	410661	PRJNA553157
SAMN12230200	M1ColonPlate1C2	M1ColonPlate1C2	mouse gut metagenome	410661	PRJNA553157
SAMN12230201	M1FecesPlate2B4	M1FecesPlate2B4	mouse gut metagenome	410661	PRJNA553157
SAMN12230202	M1FecesPlate2D4	M1FecesPlate2D4	mouse gut metagenome	410661	PRJNA553157
SAMN12230203	M1NF0Plate2A1	M1NF0Plate2A1	mouse gut metagenome	410661	PRJNA553157
SAMN12230204	M1NF0Plate2A6	M1NF0Plate2A6	mouse gut metagenome	410661	PRJNA553157
SAMN12230205	M1NF0Plate2A8	M1NF0Plate2A8	mouse gut metagenome	410661	PRJNA553157
SAMN12230206	M1NF0Plate2C2	M1NF0Plate2C2	mouse gut metagenome	410661	PRJNA553157
SAMN12230207	M1NF0Plate2C3	M1NF0Plate2C3	mouse gut metagenome	410661	PRJNA553157
SAMN12230208	M1NF0Plate2D8	M1NF0Plate2D8	mouse gut metagenome	410661	PRJNA553157
SAMN12230209	M1NF0Plate2E1	M1NF0Plate2E1	mouse gut metagenome	410661	PRJNA553157
SAMN12230210	M1NF0Plate2E3	M1NF0Plate2E3	mouse gut metagenome	410661	PRJNA553157
SAMN12230211	M1NF0Plate2F8	M1NF0Plate2F8	mouse gut metagenome	410661	PRJNA553157
SAMN12230212	M1NF0Plate2G2	M1NF0Plate2G2	mouse gut metagenome	410661	PRJNA553157
SAMN12230213	M1NF0Plate2H2	M1NF0Plate2H2	mouse gut metagenome	410661	PRJNA553157
SAMN12230214	M1NF20Plate1A11	M1NF20Plate1A11	mouse gut metagenome	410661	PRJNA553157
SAMN12230215	M1NF20Plate1A12	M1NF20Plate1A12	mouse gut metagenome	410661	PRJNA553157
SAMN12230216	M1NF20Plate1B12	M1NF20Plate1B12	mouse gut metagenome	410661	PRJNA553157
SAMN12230217	M1NF20Plate1C12	M1NF20Plate1C12	mouse gut metagenome	410661	PRJNA553157
SAMN12230218	M1NF20Plate1G12	M1NF20Plate1G12	mouse gut metagenome	410661	PRJNA553157
SAMN12230219	M1NF20Plate2A2	M1NF20Plate2A2	mouse gut metagenome	410661	PRJNA553157
SAMN12230220	M1NF20Plate2C8	M1NF20Plate2C8	mouse gut metagenome	410661	PRJNA553157
SAMN12230221	M1NF20Plate2D7	M1NF20Plate2D7	mouse gut metagenome	410661	PRJNA553157
SAMN12230222	M1NF20Plate2F1	M1NF20Plate2F1	mouse gut metagenome	410661	PRJNA553157
SAMN12230223	M1NF20Plate2F2	M1NF20Plate2F2	mouse gut metagenome	410661	PRJNA553157
SAMN12230224	M1NF20Plate2F3	M1NF20Plate2F3	mouse gut metagenome	410661	PRJNA553157
SAMN12230225	M1NF20Plate2F7	M1NF20Plate2F7	mouse gut metagenome	410661	PRJNA553157
SAMN12230226	M2ColonPlate1B2	M2ColonPlate1B2	mouse gut metagenome	410661	PRJNA553157

Continued

SAMN12230227	M2ColonPlate1F1	M2ColonPlate1F1	mouse gut metagenome	410661	PRJNA553157
SAMN12230228	M2FecesPlate1C3	M2FecesPlate1C3	mouse gut metagenome	410661	PRJNA553157
SAMN12230229	M2FecesPlate1H1	M2FecesPlate1H1	mouse gut metagenome	410661	PRJNA553157
SAMN12230230	M2NF0Plate1D11	M2NF0Plate1D11	mouse gut metagenome	410661	PRJNA553157
SAMN12230231	M2NF0Plate1H10	M2NF0Plate1H10	mouse gut metagenome	410661	PRJNA553157
SAMN12230232	M2NF0Plate1H11	M2NF0Plate1H11	mouse gut metagenome	410661	PRJNA553157
SAMN12230233	M2NF0Plate2B6	M2NF0Plate2B6	mouse gut metagenome	410661	PRJNA553157
SAMN12230234	M2NF0Plate2C9	M2NF0Plate2C9	mouse gut metagenome	410661	PRJNA553157
SAMN12230235	M2NF0Plate2D9	M2NF0Plate2D9	mouse gut metagenome	410661	PRJNA553157
SAMN12230236	M2NF0Plate2E2	M2NF0Plate2E2	mouse gut metagenome	410661	PRJNA553157
SAMN12230237	M2NF0Plate2E4	M2NF0Plate2E4	mouse gut metagenome	410661	PRJNA553157
SAMN12230238	M2NF0Plate2E7	M2NF0Plate2E7	mouse gut metagenome	410661	PRJNA553157
SAMN12230239	M2NF0Plate2E8	M2NF0Plate2E8	mouse gut metagenome	410661	PRJNA553157
SAMN12230240	M2NF0Plate2E9	M2NF0Plate2E9	mouse gut metagenome	410661	PRJNA553157
SAMN12230241	M2NF0Plate2H6	M2NF0Plate2H6	mouse gut metagenome	410661	PRJNA553157
SAMN12230242	M2NF20Plate1E12	M2NF20Plate1E12	mouse gut metagenome	410661	PRJNA553157
SAMN12230243	M2NF20Plate1F10	M2NF20Plate1F10	mouse gut metagenome	410661	PRJNA553157
SAMN12230244	M2NF20Plate2A7	M2NF20Plate2A7	mouse gut metagenome	410661	PRJNA553157
SAMN12230245	M2NF20Plate2B7	M2NF20Plate2B7	mouse gut metagenome	410661	PRJNA553157
SAMN12230246	M2NF20Plate2C6	M2NF20Plate2C6	mouse gut metagenome	410661	PRJNA553157
SAMN12230247	M2NF20Plate2C7	M2NF20Plate2C7	mouse gut metagenome	410661	PRJNA553157
SAMN12230248	M2NF20Plate2D1	M2NF20Plate2D1	mouse gut metagenome	410661	PRJNA553157
SAMN12230249	M2NF20Plate2D3	M2NF20Plate2D3	mouse gut metagenome	410661	PRJNA553157
SAMN12230250	M2NF20Plate2E6	M2NF20Plate2E6	mouse gut metagenome	410661	PRJNA553157
SAMN12230251	M2NF20Plate2G6	M2NF20Plate2G6	mouse gut metagenome	410661	PRJNA553157
SAMN12230252	M2NF20Plate2H3	M2NF20Plate2H3	mouse gut metagenome	410661	PRJNA553157
SAMN12230253	M3ColonPlate1B7	M3ColonPlate1B7	mouse gut metagenome	410661	PRJNA553157
SAMN12230254	M3ColonPlate1D6	M3ColonPlate1D6	mouse gut metagenome	410661	PRJNA553157
SAMN12230255	M3FecesPlate1A7	M3FecesPlate1A7	mouse gut metagenome	410661	PRJNA553157
SAMN12230256	M3FecesPlate1B6	M3FecesPlate1B6	mouse gut metagenome	410661	PRJNA553157
SAMN12230257	M3NF0Plate1D2	M3NF0Plate1D2	mouse gut metagenome	410661	PRJNA553157
SAMN12230258	M3NF0Plate1G4	M3NF0Plate1G4	mouse gut metagenome	410661	PRJNA553157
SAMN12230259	M3NF0Plate2A11	M3NF0Plate2A11	mouse gut metagenome	410661	PRJNA553157
SAMN12230260	M3NF0Plate2C11	M3NF0Plate2C11	mouse gut metagenome	410661	PRJNA553157
SAMN12230261	M3NF0Plate2C5	M3NF0Plate2C5	mouse gut metagenome	410661	PRJNA553157
SAMN12230262	M3NF0Plate2D11	M3NF0Plate2D11	mouse gut metagenome	410661	PRJNA553157
SAMN12230263	M3NF0Plate2E11	M3NF0Plate2E11	mouse gut metagenome	410661	PRJNA553157

Continued

SAMN12230264	M3NF0Plate2E12	M3NF0Plate2E12	mouse gut metagenome	410661	PRJNA553157
SAMN12230265	M3NF0Plate2F4	M3NF0Plate2F4	mouse gut metagenome	410661	PRJNA553157
SAMN12230266	M3NF0Plate2H11	M3NF0Plate2H11	mouse gut metagenome	410661	PRJNA553157
SAMN12230267	M3NF0Plate2H4	M3NF0Plate2H4	mouse gut metagenome	410661	PRJNA553157
SAMN12230268	M3NF20Plate1A1	M3NF20Plate1A1	mouse gut metagenome	410661	PRJNA553157
SAMN12230269	M3NF20Plate1B1	M3NF20Plate1B1	mouse gut metagenome	410661	PRJNA553157
SAMN12230270	M3NF20Plate1B4	M3NF20Plate1B4	mouse gut metagenome	410661	PRJNA553157
SAMN12230271	M3NF20Plate1B5	M3NF20Plate1B5	mouse gut metagenome	410661	PRJNA553157
SAMN12230272	M3NF20Plate1C1	M3NF20Plate1C1	mouse gut metagenome	410661	PRJNA553157
SAMN12230273	M3NF20Plate1C5	M3NF20Plate1C5	mouse gut metagenome	410661	PRJNA553157
SAMN12230274	M3NF20Plate1D1	M3NF20Plate1D1	mouse gut metagenome	410661	PRJNA553157
SAMN12230275	M3NF20Plate1D5	M3NF20Plate1D5	mouse gut metagenome	410661	PRJNA553157
SAMN12230276	M3NF20Plate1E5	M3NF20Plate1E5	mouse gut metagenome	410661	PRJNA553157
SAMN12230277	M3NF20Plate1F5	M3NF20Plate1F5	mouse gut metagenome	410661	PRJNA553157
SAMN12230278	M3NF20Plate1G3	M3NF20Plate1G3	mouse gut metagenome	410661	PRJNA553157
SAMN12230279	M3NF20Plate1G5	M3NF20Plate1G5	mouse gut metagenome	410661	PRJNA553157
SAMN12230280	M3ColonPlate1C6	M3ColonPlate1C6	mouse gut metagenome	410661	PRJNA553157
SAMN12230281	M4ColonPlate1H6	M4ColonPlate1H6	mouse gut metagenome	410661	PRJNA553157
SAMN12230282	M3FecesPlate1E7	M3FecesPlate1E7	mouse gut metagenome	410661	PRJNA553157
SAMN12230283	M4FecesPlate1G7	M4FecesPlate1G7	mouse gut metagenome	410661	PRJNA553157
SAMN12230284	M4NF0Plate1A10	M4NF0Plate1A10	mouse gut metagenome	410661	PRJNA553157
SAMN12230285	M4NF0Plate1A8	M4NF0Plate1A8	mouse gut metagenome	410661	PRJNA553157
SAMN12230286	M4NF0Plate1A9	M4NF0Plate1A9	mouse gut metagenome	410661	PRJNA553157
SAMN12230287	M4NF0Plate1B10	M4NF0Plate1B10	mouse gut metagenome	410661	PRJNA553157
SAMN12230288	M4NF0Plate1B8	M4NF0Plate1B8	mouse gut metagenome	410661	PRJNA553157
SAMN12230289	M4NF0Plate1D9	M4NF0Plate1D9	mouse gut metagenome	410661	PRJNA553157
SAMN12230290	M4NF0Plate1E8	M4NF0Plate1E8	mouse gut metagenome	410661	PRJNA553157
SAMN12230291	M4NF0Plate1F11	M4NF0Plate1F11	mouse gut metagenome	410661	PRJNA553157
SAMN12230292	M4NF0Plate1F2	M4NF0Plate1F2	mouse gut metagenome	410661	PRJNA553157
SAMN12230293	M4NF0Plate1F9	M4NF0Plate1F9	mouse gut metagenome	410661	PRJNA553157
SAMN12230294	M4NF0Plate1G9	M4NF0Plate1G9	mouse gut metagenome	410661	PRJNA553157
SAMN12230295	M4NF0Plate1H2	M4NF0Plate1H2	mouse gut metagenome	410661	PRJNA553157
SAMN12230296	M4NF20Plate2A12	M4NF20Plate2A12	mouse gut metagenome	410661	PRJNA553157
SAMN12230297	M4NF20Plate2B10	M4NF20Plate2B10	mouse gut metagenome	410661	PRJNA553157
SAMN12230298	M4NF20Plate2B12	M4NF20Plate2B12	mouse gut metagenome	410661	PRJNA553157
SAMN12230299	M4NF20Plate2C12	M4NF20Plate2C12	mouse gut metagenome	410661	PRJNA553157
SAMN12230300	M4NF20Plate2D12	M4NF20Plate2D12	mouse gut metagenome	410661	PRJNA553157

Continued

SAMN12230301	M4NF20Plate2F11	M4NF20Plate2F11	mouse gut metagenome	410661	PRJNA553157
SAMN12230302	M4NF20Plate2F12	M4NF20Plate2F12	mouse gut metagenome	410661	PRJNA553157
SAMN12230303	M4NF20Plate2G10	M4NF20Plate2G10	mouse gut metagenome	410661	PRJNA553157
SAMN12230304	M4NF20Plate2G11	M4NF20Plate2G11	mouse gut metagenome	410661	PRJNA553157
SAMN12230305	M4NF20Plate2G12	M4NF20Plate2G12	mouse gut metagenome	410661	PRJNA553157
SAMN12230306	M4NF20Plate2H10	M4NF20Plate2H10	mouse gut metagenome	410661	PRJNA553157
SAMN12230307	M4NF20Plate2H12	M4NF20Plate2H12	mouse gut metagenome	410661	PRJNA553157
SAMN12230308	M4ColonPlate1A6	M4ColonPlate1A6	mouse gut metagenome	410661	PRJNA553157
SAMN12230309	M4FecesPlate1E11	M4FecesPlate1E11	mouse gut metagenome	410661	PRJNA553157

Supplemental Table S3. Results of the pairwise PERMANOVA tests.

Comparison	Pseudo-F	*P*-value
M1 Feces *vs* M2 Feces	3.16	0.32
M1 Feces *vs* M3 Feces	2.75	0.34
M1 Feces *vs* M4 Feces	2.60	0.31
M2 Feces *vs* M3 Feces	3.15	0.33
M2 Feces *vs* M4 Feces	2.8	0.34
M3 Feces *vs* M4 Feces	3.01	0.30
M1 Colon *vs* M2 Colon	1.47	0.34
M1 Colon *vs* M3 Colon	1.46	0.34
M1 Colon *vs* M4 Colon	1.40	0.33
M2 Colon *vs* M3 Colon	1.39	0.31
M2 Colon *vs* M4 Colon	1.29	0.33
M3 Colon *vs* M4 Colon	1.41	0.33

Supplemental Table S4. Results of the Dunn's post-hoc test. Pooled microbiome refers to the pooled feces and colon samples for all mice. Comparisons are based on each 12 well plate, incubated in one of two incubators, compared to the microbiome.

Comparison	z-score	*P*-value
M1 0% *vs* Pooled microbiome	−0.54	1
M1 20% *vs* Pooled microbiome	0.92	1
M2 0% *vs* Pooled microbiome	−1.02	1
M2 20% *vs* Pooled microbiome	0.66	1
M3 0% *vs* Pooled microbiome	−3.81	0.01
M3 20% *vs* Pooled microbiome	3.21	0.02
M4 0% *vs* Pooled microbiome	4.07	0.01
M4 20% *vs* Pooled microbiome	5.41	0.01

Supplemental Table S5. Results of the pairwise PERMANOVA test.

Comparison	Pseudo-F	*P*-value
pH 6 *vs* pH 7	1.86	0.04
pH 6 *vs* pH 9	17.15	0.01
pH 6 *vs* pH 10	25.46	0.01
pH 7 *vs* pH 9	15.27	0.01
pH 7 *vs* pH 10	22.31	0.01
pH 9 *vs* pH 10	1.62	0.03

Supplemental Table S6. Hypothesis testing for sources of variation by distance-based linear modeling. Abbreviations: df, degrees of freedom; SS, sum of squares; Prop, proportion of variation.

Source	SS	Pseudo-F	*P* (perm)	Prop.
Oxygen	3437.2	1.2965	0.171	0.14047
pH	50147	23.457	0.001	0.20494
Mouse	44634	20.303	0.001	0.18241
Sibling Relationship	53679	25.573	0.001	0.21938

Supplemental Table S7. Results of Dunn's test for each mouse comparison.

Comparison	z-score	*P*-value
M1 *vs* M2	0.51	0.30
M1 *vs* M3	4.51	0.01
M1 *vs* M4	6.27	0.01
M2 *vs* M3	4.00	0.01
M2 *vs* M4	0.57	0.01
M3 *vs* M4	1.67	0.094

Supplemental Table S8. Results of the comparison of *Enterococcus* between plates and the pooled microbiome. Results generated from a non-parametric t-test using 1000 permutations.

Comparison	t-score	*P*-value
M1 0% *vs* Pooled microbiome	2.37	0.01
M1 20% *vs* Pooled microbiome	2.37	0.01
M2 0% *vs* Pooled microbiome	2.91	0.01
M2 20% *vs* Pooled microbiome	4.77	0.01
M3 0% vs Pooled microbiome	10.48	0.01
M3 20% vs Pooled microbiome	6.00	0.01
M4 0% vs Pooled microbiome	7.97	0.01
M4 20% vs Pooled microbiome	13.65	0.01

Supplemental Table S9. Results of the comparison between strains of Proteobacteria, *Enterococcus*, *Lactobacillus*, and Archaea between mice. Results generated from a non-parametric t-test using 1000 permutations.

Comparison	Strain	t-score	*P*-value
pH 6 *vs* pH 7	Proteobacteria	1.11	0.14
	Enterococcus	0.10	0.31
	Lactobacillus	3.96	0.01
	Archaea	1.19	0.47
pH 6 *vs* pH 9	Proteobacteria	−1.71	0.08
	Enterococcus	7.16	0.01
	Lactobacillus	2.86	0.01
	Archaea	2.67	0.01
pH 6 *vs* pH 10	Proteobacteria	−3.43	0.01
	Enterococcus	9.02	0.01
	Lactobacillus	3.16	0.01
	Archaea	3.47	0.01
pH 7 *vs* pH 9	Proteobacteria	−5.03	0.01
	Enterococcus	6.30	0.01
	Lactobacillus	0.54	0.66
	Archaea	2.71	0.01
pH 7 *vs* pH 10	Proteobacteria	−7.57	0.01
	Enterococcus	7.19	0.01
	Lactobacillus	0.48	0.73
	Archaea	3.49	0.01
pH 9 *vs* pH 10	Proteobacteria	−2.31	0.02
	Enterococcus	0.83	0.55
	Lactobacillus	0.11	0.92
	Archaea	1.53	0.13

Supplemental Table S10. Results of the comparison. Results generated from a non-parametric t-test using 1000 permutations.

Comparison	t-score	*P*-value
M1 *vs* M2	0.089	0.38
M1 *vs* M3	3.31	0.01
M1 *vs* M4	4.12	0.01
M2 *vs* M3	2.80	0.01
M2 *vs* M4	3.22	0.01
M3 *vs* M4	1.89	0.07